Journal of Applied Polymer Science

Freestanding Ag_2S/CuS PVA films with improved dielectric properties for organic electronics

Ann Mary K. Aippunny,[1,2] Sajna M. Shamsudeen,[1] Prakashan Valparambil,[1] Siby Mathew,[3] Unnikrishnan N. Vishwambharan[1]

[1]School of Pure and Applied Physics, Mahatma Gandhi University, Kottayam, Kerala 686 560, India
[2]Department of Physics, St. Thomas' College (Autonomous), Thrissur, Kerala 680 001, India
[3]Department of Physics, S.H. College (Autonomous), Thevara, Kerala 682 013, India
Correspondence to: U. N. Vishwambharan (E-mail: nvu100@yahoo.com)

ABSTRACT: The prime goal of this work is to synthesize free-standing polyvinyl alcohol (PVA) films doped with Ag_2S, CuS, Ag_2S/CuS alloy, and Ag_2S/CuS nanocomposites through the sol–gel route. The dependence of Ag_2S content in the PVA nanocomposite films on both the real and imaginary parts of the complex permittivity and loss tangent values was examined. An enhanced dielectric constant was achieved with minimum dielectric loss due to the insulating silica layer. By changing the Ag_2S content in Ag_2S/CuS PVA films, the AC conductivity is improved with pure Ag_2S nanoparticles exhibiting highest values of the order of $10^{-6}-10^{-9}$ S/cm. The Cole–Cole parameters were calculated and the semicircles observed in the plots indicate a single relaxation process. The results suggest that these composite films are potential materials for embedded capacitor applications. © 2016 Wiley Periodicals, Inc. J. Appl. Polym. Sci. **2016**, *133*, 43568.

KEYWORDS: composites; dielectric properties; nanostructured polymers; synthesis and processing

Received 14 October 2015; accepted 21 February 2016
DOI: 10.1002/app.43568

INTRODUCTION

In recent years intensive research activities in the fabrication of polymer nanocomposites are progressing in an increasing pace for developing high dielectric materials for integrated electronic circuits and microelectronics. High dielectric materials with tunable dielectric properties are inevitable for high charge storage capacitors and electronic devices.[1,2] By introducing inorganic nanofillers, the physicochemical properties of the system can be modified. Even though conventional fabrication of ferroelectric metal oxide polymer composites[3] promises high-ε_r composite materials, conducting nanofillers including carbon nanotubes,[4] graphene nanostructures,[5] and metal-semiconductor nanoparticles[6] are being employed now a days to improve flexibility and processability. The frequency dependence of ac-conductivity and dielectric constant of the PVA–PbS nanocomposite[7] and p-type (PVA/CuI) nanocomposite polymer[8] has been carried out earlier with the aid of complex/dielectric spectroscopic investigations. Silica glasses doped with varying contents of CdSe nanocrystallites are prepared by the sol–gel exhibited the conductivity values of the order of $10^{-5}-10^{-7}$ S/cm.[9] Moreover, superior dielectric behavior of the multiwalled carbon nanotube-CdS/polyvinyl alcohol (MWCNT-CdS/PVA) composites over MWCNT and PVA host matrices has been demonstrated.[10] Though significant efforts have been focused on developing various polymer-conductive nanofillers composites using silver (Ag), aluminum (Al), and nickel (Ni) as conducting fillers, they are accompanied with high dielectric loss tangent.[11–16] One can achieve a significant change in dielectric properties of polymer composites through incorporation of conducting nanofillers with low threshold volume fraction.[6,17] Usually investigations on tuning and improving dielectric parameters are done by varying content of conducting fillers, where a higher value of dielectric constant is reached when volume fraction approaches the percolation threshold.[5] Fabrication of materials with high dielectric constant having tunable dielectric value by varying the constituent nanocrystal stoichiometries not only would be attractive for fundamental physics but also has considerable interest in different fields of application. The incorporation of these nanostructures as conducting fillers is not very well explored. By using nanocomposites of different semiconductors as conducting fillers, in addition to content dependent dielectric performance of the matrix, one can possibly improve the dielectric constant by varying constituent nanocrystal stoichiometry and content.

Despite the tailoring of dielectric properties of a polymer or glass matrix by varying the content of the conducting nanofillers, their applicability remains fairly limited because of their poor compatibility with nanofillers. The nanoparticles are not well dispersed unless they are surface functionalized or capped with suitable hydrophilic agents. Recently many researchers focused on controlled dispersion

of nanomaterials in polymer matrix through modification of their surface with silica resulting in the formation of stable intermolecular hydrogen bonding between oxygen atom of SiO_2 chain and hydroxyl group of polymer chain.[18–20] This could afford strong interaction between nanomaterials and polymer forming stable dispersion of nanomaterials in polymer host. Among the well-studied semiconductor nanoparticles, CuS and Ag_2S stand out as NIR materials with nontoxic nature compared to the chalcogenide nanoparticles of cadmium, lead, and mercury.[21,22] Owing to the size and composition tunable optical and electrical properties, considerable research on semiconductor–semiconductor alloy/nanocomposite systems is evolving for realization in high photocatalytic activity, efficient solar energy conversion and nonlinear optics.[23–25] Recently, we have reported the synthesis of Ag_2S/CuS alloy/nanocomposite systems with their nonlinear optical properties being improved by the relative amount of Ag_2S in the nanomaterial.[26]

In this work, silica-capped Ag_2S, CuS, Ag_2S/CuS alloy, and Ag_2S/CuS nanocomposite particles were used as conducting fillers to significantly improve the dielectric parameters of PVA polymer nanocomposites prepared by simple sol–gel route. The detailed FTIR analysis shows that silica is linked to PVA through intermolecular hydrogen bonds forming a stable dispersion of nanofillers in the polymer matrix. Frequency-dependent AC conductivity and dielectric response were recorded at room temperature for a frequency range of 100 Hz–2 MHz. The dielectric relaxation process is examined from the Nyquist diagram and the nature of electrical conduction is determined from the low-frequency data.

EXPERIMENTAL

Materials

Copper(II) acetate monohydrate $Cu(CO_2CH_3)_2{\cdot}H_2O$, copper(II) nitrate trihydrate $Cu(NO_3)_2{\cdot}3H_2O$, silver nitrate ($AgNO_3$), thioacetamide (CH_3CSNH_2), and poly(vinyl alcohol) $[–CH_2CHOH–]_n$ were obtained from Sigma–Aldrich as analytical grade. Tetraethyl orthosilicate ($C_8H_{20}O_4Si$), nitric acid (HNO_3), and ethanol were bought from Merck India. All chemicals were used as received without further purification.

Preparation

Usually, silica-capped nanoparticles are prepared through Stober method[27–29] and reverse micoemulsion method[30,31] which involves multiple complicated steps. The silica-capped Ag_2S, CuS, Ag_2S/CuS alloy, and Ag_2S/CuS nanocomposite particles were synthesized through a sol–gel process with tetraethyl orthosilicate (TEOS) as precursors in the presence of ethanol.[26] The dopants were added in the form of copper acetate and copper nitrate, silver nitrate, and thioacetamide as copper, silver, and sulfur sources, respectively. A measured volume of 1 *M* HNO_3 was added as catalyst.

PVA nanocomposites of 3 wt % nanofillers were prepared from sol–gel synthesis at room temperature. In a typical procedure for preparing CuS/PVA films, 0.2 g of PVA is dissolved in 10 mL distilled water and required amount of CuS nanopartilces was introduced into the PVA solution. Further required amount of different Ag_2S, Ag_2S/CuS alloy, and Ag_2S/CuS nanocomposite particles were used as nanofillers for preparing the three other PVA nanocomposite films. The solution was stirred for 1 h to obtain a homogenous mixture. The solution was cast into a polypropylene dish and was kept at 50 °C for 2 days. The thin films peeled off from the polypropylene dish were used for further investigations.

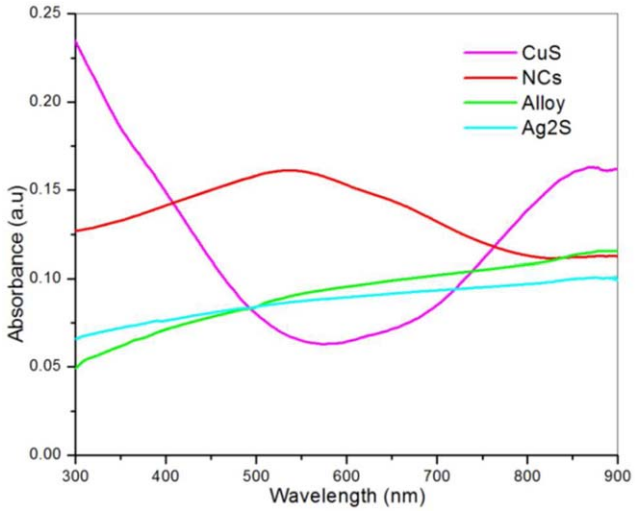

Figure 1. Absorption spectra of PVA films doped with CuS, Ag_2S, Ag_2S–CuS alloy and CuS–Ag_2S nanocomposites. [Color figure can be viewed in the online issue, which is available at wileyonlinelibrary.com.]

Characterization Methods

The optical spectra of the samples were recorded with UV–Vis spectrometer (Perkin Elmer, Lambda 35). The FTIR spectrum was recorded using a Shimadzu 8400S Spectrophotometer to analyze the effect of capping agents. By using the Agilent Impedance Analyzer (model E4980A), parameters like complex impedance, AC conductivity, and dielectric relaxation were measured in the frequency range of 100 Hz–2 MHz, by the dielectric spectroscopic technique. The PVA nanocomposite films were cut into circular pieces with 1 cm diameter and conducting silver paste is applied to both faces to form the electrodes in contact with the two circular faces. The thickness of the films measured using screw gauge is in the range of 0.08–1.1 mm. The film was sandwiched between two stainless disc electrodes of a sample holder and was connected to the impedance spectrometer for data acquisition to examine their dielectric properties. The information regarding crystallinity, purity and TEM images have been reported in one of our earlier communications.[26]

RESULTS AND DISCUSSION

UV–visible absorption spectra (Figure 1) reveal two absorption band for CuS-PVA films; one related to exciton absorption at lower energy and the other related to plasmon absorption at near infrared (NIR) range. The characteristic NIR absorption band of CuS nanocrystallites is attributed to strong free carrier absorption by holes due to increased copper vacancies.[22] The narrow band gap semiconductor, Ag_2S nanocrystallites, has a broad absorption in the visible region and Ag_2S/CuS alloy PVA films have similar absorption band with that of Ag_2S. The Ag_2S/CuS nanocomposite PVA films have an absorption peak at 541 nm and their steady-state absorption characteristics are different from PVA films doped with CuS nanoparticles or Ag_2S nanoparticles.

FTIR is used to testify the interaction of PVA with the surface of silica-capped nanofillers. As shown in Figure 2, PVA has two characteristic peaks at around 2900 and 1700 cm^{-1} which are associated with vibration modes of —CH_2 and C═O groups.[9] The C═O groups are present in unhydrolysed PVA, containing O—H vibrations. This O—H stretching vibration results in a band at 3302 cm^{-1} which may also has contributions from stable intermolecular hydrogen bonding between oxygen atom of SiO_2 chain and hydroxyl group of polymer chain. The —OH peaks observed in the FTIR spectra of the nanocomposite films indicate the probability that some of the —OH groups, either from silanol or PVA, are not consumed in cross-linking. The C—OH vibrations present in PVA peaked at 1091 cm^{-1} become broader and intense for PVA nanocomposite films which can be attributed to overlapping of Si—O—Si with the C—C—O vibrations. The presence of Si—O—C vibrations reported to be at 1100 cm^{-1} can also interfere with C—O stretching movement of PVA and asymmetric Si—O—Si stretching band.[32] These results indicate that the surface treatment of the nanoparticles with silica could endow the strong interaction and cross-linking between PVA and silica-capped nanoparticles resulting in their stable dispersion in polymer host.

To measure the dielectric and conductivity properties of a material, sinusoidal voltages of different frequencies were applied across the sample of thickness d and area A. The real part of dielectric constant can be computed at the various frequencies by using the measured capacitance values "C_p" using the relation

$$\varepsilon'(\omega)=\frac{C_p d}{\varepsilon_0 A} \tag{1}$$

The imaginary part of dielectric constant and the loss tangent or dissipation factor is defined by the following equation

$$\tan\delta=\frac{\varepsilon''}{\varepsilon'} \tag{2}$$

where ε_0 is the permittivity of free space, C_p is the parallel capacitance across the sample, and $\tan\delta$ $[=1/\tan\theta]$ represents the loss tangent or dissipation factor.

The ac conductivity can be expressed as

$$\sigma_{ac}=\omega\varepsilon_0\varepsilon'' \tag{3}$$

$$\sigma_{ac}=2\pi f\ \varepsilon_0\varepsilon'\ \tan\delta \tag{4}$$

where ω $(=2\pi f)$ represents the angular frequency of the sinusoidal signal.[33]

Jonscher proposed an appropriate formalism to explore the dependence of frequency on conductivity in a material known as power–law relation[34] and is given by

$$\sigma_T(\omega)=\sigma_0+A\omega^s \tag{5}$$

where coefficient A and exponent s are temperature- and material-dependent parameters, $\sigma_T(\omega)$ is the frequency-dependent total conductivity and σ_0 is the frequency-independent dc conductivity. The second term on the RHS of eq. (5) indicates the frequency-dependent ac conductivity (σ_{ac}) and is attributed to the reduction in dielectric values resulting from the localized electric charge carriers.

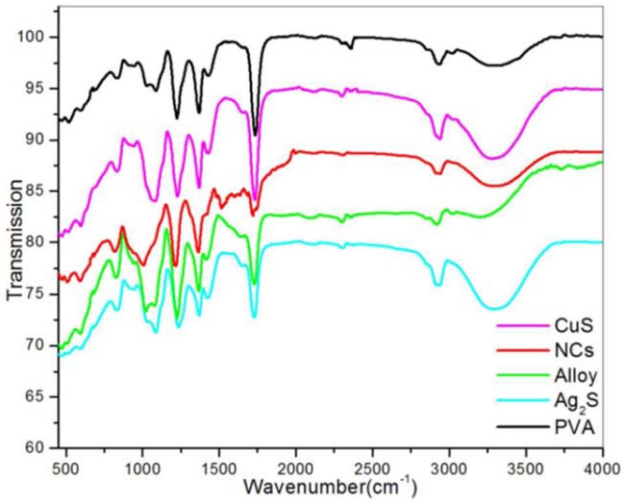

Figure 2. FTIR spectra of PVA films doped with CuS, Ag_2S, Ag_2S–CuS alloy, and CuS–Ag_2S nanocomposites. [Color figure can be viewed in the online issue, which is available at wileyonlinelibrary.com.]

In general, the value of universal power–law exponent (s) is always such that $0\leq s\leq 1$ and is a measure of degree of correlation among frequency (f) and conductivity (σ_{ac}). As correlation increases, the s value tends to unity and a zero value of s indicates the random hopping of electrons.

Real (Z') and imaginary (Z'') parts of impedance can be expressed as

$$Z'=|Z|\cos\theta \tag{6}$$

$$Z''=|Z|\sin\theta \tag{7}$$

where θ $[=\tan^{-1}(Z''/Z')]$ is the phase angle.

The low-frequency intercept on the real impedance axis made by the semicircle is used to calculate the frequency-independent dc resistance (R_b) of the samples and the peaks of the semicircles are utilized to investigate the values of relaxation time (τ). The bulk capacitance, C_b can be calculated using the expression

$$C_b=\frac{1}{2\pi f_p R_b} \tag{8}$$

and the relaxation time, τ is represented as

$$\tau=R_b C_b=\frac{1}{2\pi f_p} \tag{9}$$

The frequency dependence of real and imaginary part of dielectric constant is shown in Figure 3. With the addition of nanofillers, the dielectric constant of the PVA films is found to improve greatly because of the formation of microcapacitor network consisting of nanoparticles separated by the PVA dielectric layer. The dielectric constant of the composites decreases with increasing frequency at low-frequency region. This can be better explained by Maxwell–Wagner–Sillars (MWS) polarization or interfacial polarization. The accumulation of charge carriers at the interface between polymer and nanofiller in an external applied electric field can cause interfacial polarization. The frequency dependent behavior of the dielectric constants in the

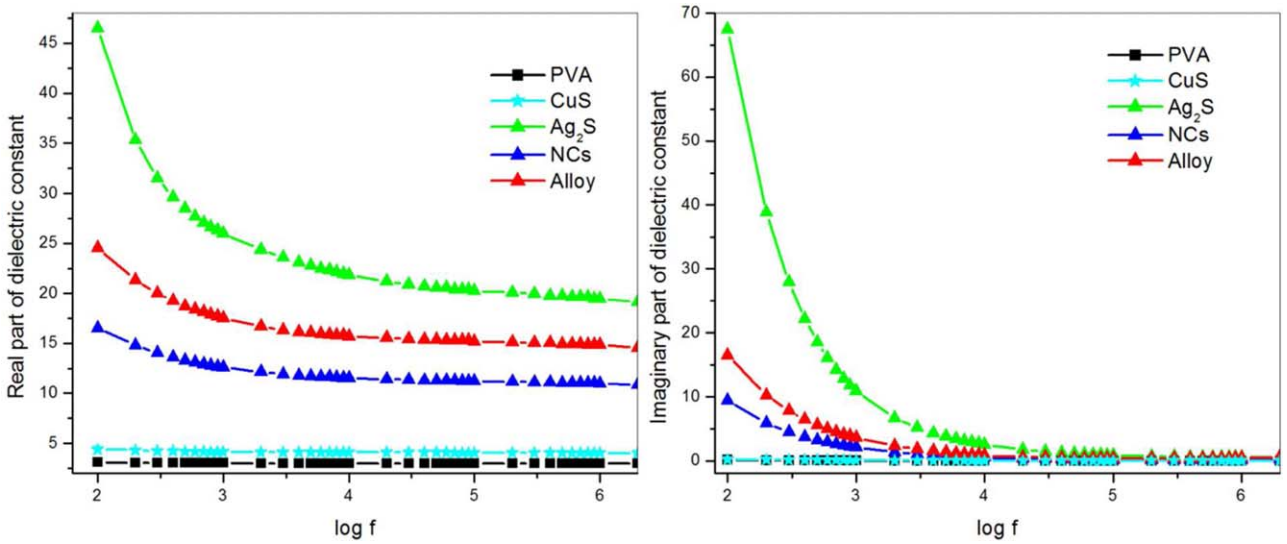

Figure 3. Variation of (a) real and (b) imaginary part of dielectric constant with frequency. [Color figure can be viewed in the online issue, which is available at wileyonlinelibrary.com.]

low-frequency range demonstrated a strong MWS polarization in nanocomposites of poly-vinylidene fluoride incorporated with reduced graphene oxide and poly-vinyl alcohol.[17]

CuS is known to have excess of holes due to copper vacancies and when an external field is applied, more dipoles are developed due to the trapped charge carriers and space charge distribution at interfaces. But the frequency dependence of dielectric constant is small for CuS-doped nanocomposites, while for Ag_2S, the dielectric behavior decreases exponentially with increase in frequency. Though migration and accumulation of holes in CuS needs a relatively longer time, Ag_2S nanoparticles have more electrons as free carriers with higher mobility and ionic conductivity. Thus, the dielectric value remains higher as expected (above 20) for Ag_2S-doped film even at higher frequencies as compared to other PVA nanocomposite films. On close observation, it can be inferred that the dielectric constant becomes almost constant at higher frequencies and dominant polarization mechanism is orientational polarization. Since the nanofillers are silica-capped nanoparticles, charge carriers are bounded and needs more time for migration and accumulation at the interfaces. Also high dielectric loss values of polymer nanocomposites upon addition of inorganic fillers are not advantageous for materials having embedded capacitor applications.[6,35] But for silica-capped PVA nanocomposite films, the insulating silica layer prevents direct contact between conducting fillers and dielectric material. This minimizes leakage current in the composite, thereby reducing the dielectric loss. From Figure 4, it can be seen that the dielectric loss of PVA film is not enhanced at higher frequencies after introducing nanofillers while an enhanced dielectric constant is achieved at this range.

The variation of ac conductivity with "log *f*" is plotted in Figure 5. It can be seen that even though conductivity of PVA films and CuS-doped PVA films have weak dependence on frequency, the conductivity is found to increase with frequency at high-frequency

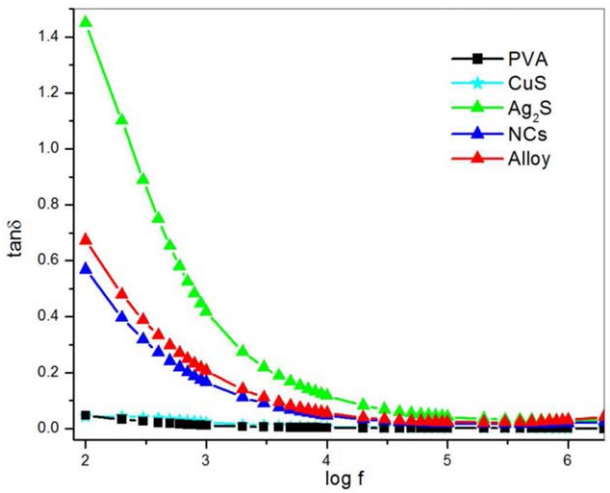

Figure 4. Variation of dielectric loss with frequency. [Color figure can be viewed in the online issue, which is available at wileyonlinelibrary.com.]

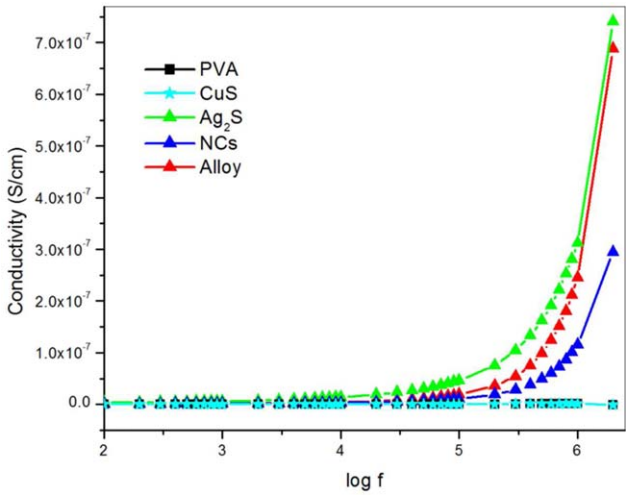

Figure 5. Variation of conductivity with frequency. [Color figure can be viewed in the online issue, which is available at wileyonlinelibrary.com.]

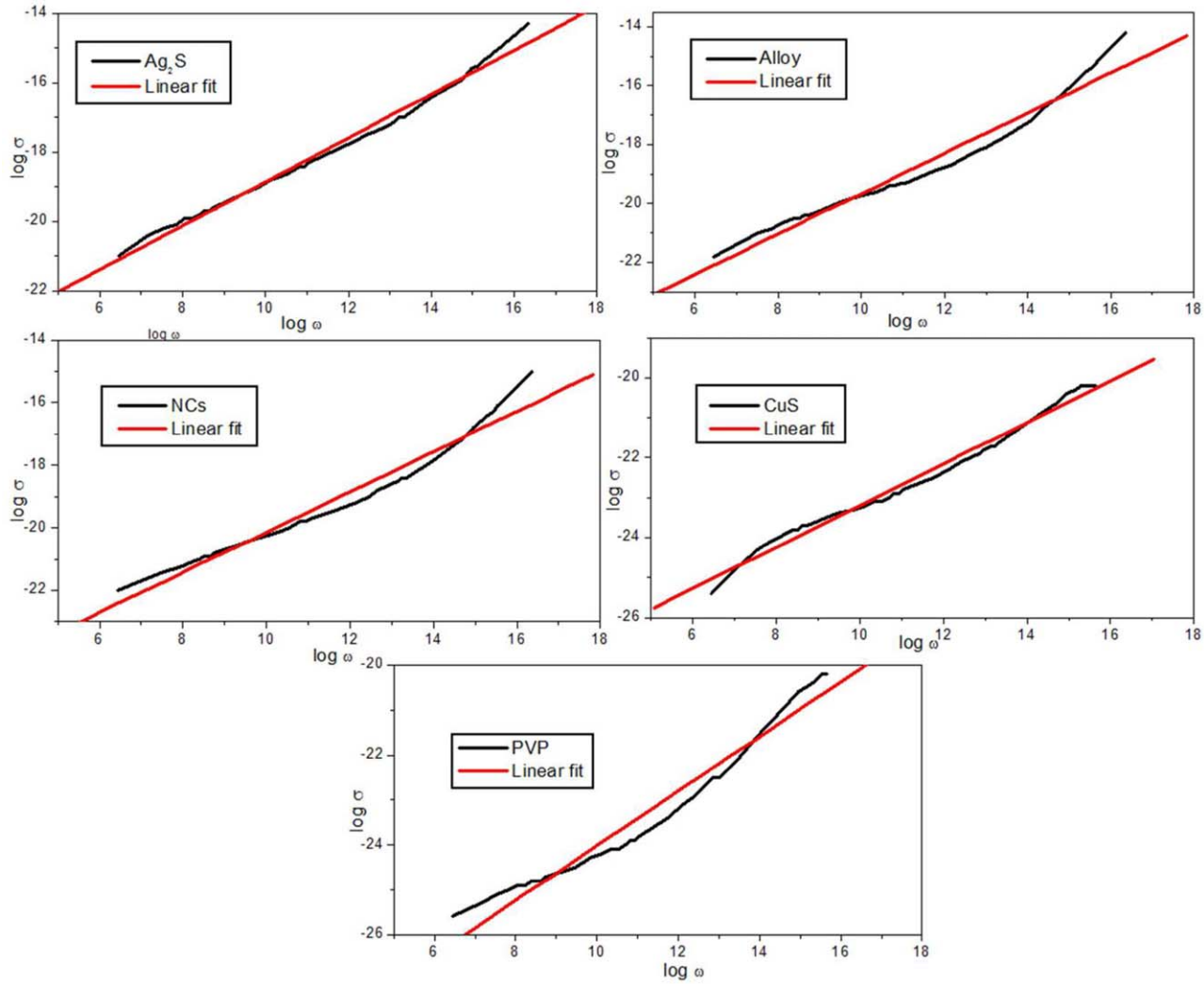

Figure 6. Linear fit to conductivity frequency logarithmic graph. [Color figure can be viewed in the online issue, which is available at wileyonlinelibrary.com.]

range for Ag_2S, alloy, and NCs-doped samples. The conductivity can be improved with relative amount of Ag_2S in the nanocomposite films, with higher conductivity for Ag_2S-doped films. The frequency-dependent conductivity is caused by the hopping of electrons in the localized states near the Fermi level and also due to the excitation of charge carriers to the states in the conduction band.

The frequency-dependent conductivity has been attributed to relaxation caused by the motion of electron, or atoms/ions, hopping or tunneling between the equilibrium sites of solids. The values of σ_0, s, and A are known as power–law parameters. The power–law parameters σ_0, s, and A obtained from the linear fit to conductivity frequency logarithmic graph (Figure 6) are tabulated in Table I. The values of the exponent s obtained using the least square fitting are in the range 0.5–0.7. The values of the parameter are closely associated with carrier transport component in the hopping conduction mechanism and obey the universal dynamic model. The values change irregularly with nanofiller content and hence depend on the composition of composite matrix. The higher value of s for PVA films with CuS–Ag_2S alloy and nanocomposites as nanofillers can be attributed to increase in content of Ag^+ ions in the PVA films. This brings about an enhancement in the ac conductivity particularly in higher frequency region, where ionic conduction is more prominent.

Table I. Power–Law Parameters for Ag_2S/CuS-Doped PVA Films

PVA film	$\sigma_0(\times10^{-11})$	s	$A(\times10^{-12})$
PVA	0.834	0.52	0.084
CuS	0.0664	0.61	0.465
CuS-Ag_2S NCs	24.9	0.64	2.88
CuS-Ag_2S alloy	56.3	0.68	3.04
Ag_2S	298	0.63	11.6

As the sample is considered to be a capacitor with dielectrics placed between the electrodes, it can be better described by a parallel resistor–capacitor equivalent circuit system with resistance

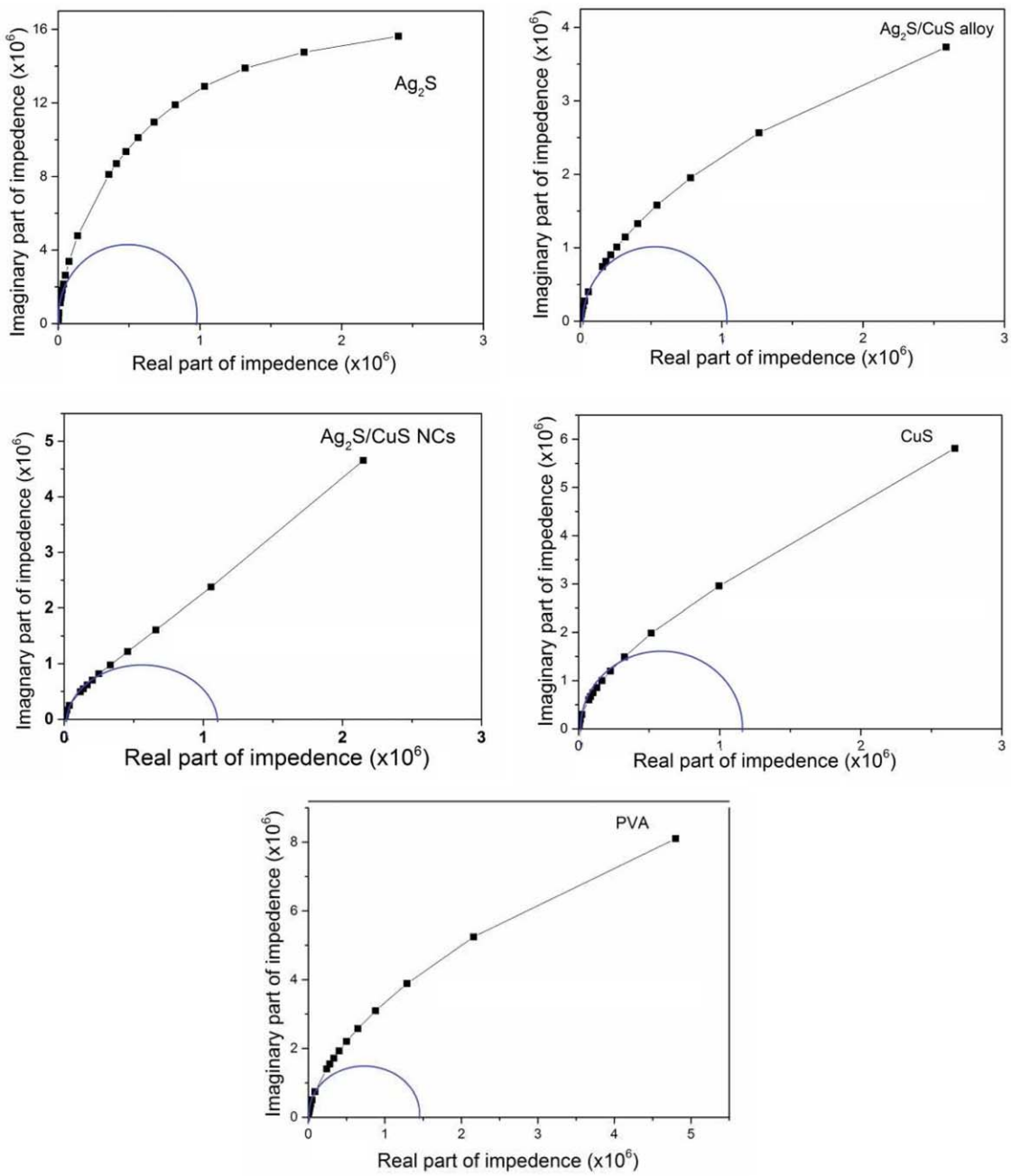

Figure 7. Complex impedance plots. [Color figure can be viewed in the online issue, which is available at wileyonlinelibrary.com.]

R_b and capacitance C_b. This "RC" element is characterized by a relaxation time, τ, which is a product of R_b and C_b. The complex impedance plots (Cole–Cole plots) of the PVA nanocomposite films are shown in Figure 7. Single semicircles observed for PVA films doped with Ag_2S, Ag_2S/CuS nanocomposites, and alloy can be modeled by an equivalent parallel RC circuit. The relaxation time and the DC (frequency-independent) resistance of the sample is determined from the peaks of the semicircles and low-frequency intercept made by the semicircle on the real impedance axis, respectively. The semicircles reveal a single relaxation process in the higher frequency region and the values of Cole–Cole parameters (values of R_b, C_b, and τ) are tabulated in Table II. The dipolar relaxation observed is associated with the dielectric property of the system. This decreases with increase in Ag_2S content of the samples with a minimum value for PVA–Ag_2S films.

Table II. Cole–Cole Parameters for PVA Nanocomposite Films

Glass code	R_b (MΩ)	C_b ($\times 10^{-4}$ μF)	τ (10^{-4} s)
Ag_2S	0.97	1.63	1.58
Ag_2S/CuS alloy	1.09	1.82	1.99
Ag_2S/CuS NCs	1.18	2.07	2.44
CuS	1.23	3.18	3.91
Pure film	1.49	3.23	4.81

CONCLUSIONS

We have synthesized free-standing PVA polymer composite films by incorporating Ag_2S/CuS nanoparticles with varying constituent composition. The silica-modified nanoparticles favor a strong interaction and cross-linking between PVA and nanoparticles. This enhances a stable dispersion of the nanoparticle in the polymer host. It is observed that the insulating silica layer prevents direct contact between conducting fillers and dielectric material, thereby minimizing leakage current in the composite. This in turn results in the dielectric loss of PVA nanocomposite films at higher frequencies, while an enhanced dielectric constant is attained in this frequency range. The dielectric constant versus frequency variation follows the Maxwell–Wagner–Sillars (MWS) polarization or interfacial polarization process. High ionic conductivity of Ag_2S promotes an enhancement in the dielectric value even at higher frequencies which decreases gradually with Ag_2S content in the PVA nanocomposite films. Similarly, the conductivity can be improved with relative amount of Ag_2S in the nanocomposite films and follows Jonscher's power–law dependence. Also the dipolar relaxation determined from the Cole–Cole plots decreases with Ag_2S content, with a minimum value for PVA films with Ag_2S as nanofillers. Thus it can be summed up that nanoparticles are suitable candidates for the improvement of the dielectric properties of a polymer material that can be used in the field of organic electronics.

ACKNOWLEDGMENTS

One of the authors (KAAM) gratefully acknowledges Kerala State Council for Science Technology and Environment for the award of Research Fellowship. SMS and PVP are thankful to UGC and KSCSTE for financial support in the form of RFSMS and Research Project Fellowships, respectively.

REFERENCES

1. Lu, J. X.; Wong, C. P. *IEEE Trans. Dielectr. Electr. Insul.* **2008**, *15*, 1322.
2. Yuan, J.-K.; Dang, Z.-M.; Yao, S.-H.; Zha, J.-W.; Zhou, T.; Li, S.-T.; Bai, J. *J. Mater. Chem.* **2010**, *20*, 2441.
3. Srivastava, R. K.; Narayanan, T. N.; Mary, A. P. R.; Anantharaman, M. R.; Srivastava, A.; Vajtai, R.; Ajayan, P. M. *Appl. Phys. Lett.* **2011**, *99*, 113116.
4. Higginbotham, A. L.; Stephenson, J. J.; Smith, R. J.; Killips, D. S.; Kempel, L. C.; Tour, J. M. *J. Phys. Chem. C* **2007**, *111*, 17751.
5. Dimiev, A.; Zakhidov, D.; Genorio, B.; Oladimeji, K.; Crowgey, B.; Kempel, L.; Rothwell, E. J.; Tour, J. M. *Appl. Mater. Interfaces* **2013**, *5*, 7567.
6. Zhang, Y.; Wang, Y.; Deng, Y.; Li, M.; Bai, J. *Appl. Mater. Interfaces* **2012**, *4*, 65.
7. Jana, S.; Thapa, R.; Maity, R.; Chattopadhyay, K. K. *Phys. E* **2008**, *40*, 3121.
8. Sheha, E.; Khoder, H.; Shanap, T. S.; El-Shaarawy, M. G.; El Mansy, M. K. *Optik* **2012**, *123*, 1161.
9. Adiyodi, A. K.; Jyothy, P. V.; Unnikrishnan, N. V. *J. Appl. Polym. Sci.* **2009**, *113*, 887.
10. Mondal, S. P.; Aluguri, R.; Ray, S. K. *J. Appl. Phys.* **2009**, *105*, 114317.
11. Wang, L.; Dang, Z. M. *Appl. Phys. Lett.* **2005**, *87*, 042903.
12. Dang, Z. M.; Wang, L.; Yin, Y.; Zhang, Q.; Lei, Q. Q. *Adv. Mater.* **2007**, *19*, 852.
13. Qi, L.; Lee, B. I.; Chen, S.; Samuels, W. D.; Exarhos, G. *J. Adv. Mater.* **2005**, *17*, 1777.
14. Lu, J.; Moon, K. S.; Xu, J.; Wong, C. P. *J. Mater. Chem.* **2006**, *16*, 543.
15. Xu, J. X.; Wong, C. P. *Appl. Phys. Lett.* **2005**, *87*, 082907.
16. Dang, Z. M.; Shen, Y.; Nan, C. W. *Appl. Phys. Lett.* **2002**, *81*, 4814.
17. Wang, D.; Bao, Y.; Zha, J.-W.; Zhao, J.; Dang, Z.-M.; Hu, G.-H. *Appl. Mater. Interfaces* **2012**, *4*, 6273.
18. Mulvaney, P.; Liz-Marza, L. M.; Giersig, M.; Ung, T. *J. Mater. Chem.* **2000**, *10*, 1259.
19. Jana, N. R.; Earhart, C.; Ying, J. Y. *Chem. Mater.* **2007**, *19*, 5074.
20. Graf, C.; Vossen, D. L. J.; Imhof, A.; Blaaderen, A. *Langmuir* **2003**, *19*, 6693.
21. Jiang, P.; Tian, Z.-Q.; Zhu, C.-N.; Zhang, Z.-L.; Pang, D.-W. *Chem. Mater.* **2012**, *24*, 3.
22. Luther, J. M.; Jain, P. K.; Ewers, T.; Alivisatos, A. P. *Nat. Mater.* **2011**, *10*, 361.
23. Xie, Y.; Heo, S. H.; Kim, Y. N.; Yoo, S. H.; Cho, S. O. *Nanotechnology* **2010**, *21*, 015703.
24. Ratanatawanate, C.; Bui, A.; Vu, K.; Balkus, K. J. *J. Phys. Chem. C* **2011**, *115*, 6175.
25. Han, M. Y.; Huang, W.; Chew, C. H.; Gan, L. M.; Zhang, X. J.; Ji, W. *J. Phys. Chem. B* **1998**, *102*, 1884.
26. Ann Mary, K. A.; Unnikrishnan, N. V.; Philip, R. *Mat. Res. Bull.* **2015**, *04*, 034.
27. Stober, W.; Fink, A.; Bohn, E. *J. Colloid Interface Sci.* **1968**, *26*, 62.
28. Yang, P.; Ando, M.; Murase, N. *J. Colloid Interface Sci.* **2007**, *316*, 420.
29. Correa-Duarte, M. A.; Giersig, M.; Liz-Marzan, L. M. *Chem. Phys. Lett.* **1998**, *286*, 497.
30. Darbandi, M.; Urban, G.; Krüger, M. *Colloid Interface Sci.* **2010**, *351*, 30.
31. Lai, C. W.; Wang, Y. H.; Chen, Y. C.; Hsieh, C. C.; Uttam, B. P.; Hsiao, J. K.; Hsu, C. C.; Chou, P. T. *J. Mater. Chem.* **2009**, *19*, 8314.
32. Pirzada, T.; Arvidson, S. A.; Saquing, C. D.; Shah, S. S.; Khan, S. A. *Langmuir* **2012**, *28*, 5834.
33. Zhang, Q. Y.; Pita, K.; Kam, C. H. *J. Phys. Chem. Solids* **2003**, *64*, 333.
34. Jonscher, K.; Andrew, J. *Phys. D Appl. Phys.* **1999**, *32*, R57.
35. Wang, G. *Appl. Mater. Interfaces* **2010**, *2*, 1290.